Cell PRESS
Open ACCESS

Cell Reports
Article

A Role of RIP3-Mediated Macrophage Necrosis in Atherosclerosis Development

Juan Lin,[1,6] Hanjie Li,[1,6] Min Yang,[2] Junming Ren,[1] Zhe Huang,[1] Felicia Han,[1] Jian Huang,[3] Jianhui Ma,[1] Duanwu Zhang,[1] Zhirong Zhang,[1] Jianfeng Wu,[1] Deli Huang,[1] Muzhen Qiao,[1] Guanghui Jin,[4] Qiao Wu,[1] Yinghui Huang,[5] Jie Du,[2,*] and Jiahuai Han[1,*]

[1]State Key Laboratory of Cellular Stress Biology and School of Life Sciences, Xiamen University, Xiamen, Fujian, China
[2]Beijing Institute of Heart, Lung and Blood Vessel Diseases, Beijing Anzhen Hospital, Capital Medical University, Beijing 100029, China
[3]The First Affiliated Hospital of Xiamen University, Xiamen, Fujian, China
[4]Department of Basic Medical Sciences, Medical College, Xiamen University, Xiamen, Fujian, China
[5]China-Japan Union Hospital, Jilin University, Changchun, Jilin, China
[6]These authors contribute equally to this work
*Correspondence: jiedu@yahoo.com (J.D.), jhan@scripps.edu (J.H.)
http://dx.doi.org/10.1016/j.celrep.2012.12.012

SUMMARY

Necrotic death of macrophages has long been known to be present in atherosclerotic lesions but has not been studied. We examined the role of receptor interacting protein (RIP) 3, a mediator of necrotic cell death, in atherosclerosis and found that *RIP3*$^{-/-}$;*Ldlr*$^{-/-}$ mice were no different from *RIP3*$^{+/+}$;*Ldlr*$^{-/-}$ mice in early atherosclerosis but had significant reduction in advanced atherosclerotic lesions. Similar results were observed in *Apoe*$^{-/-}$ background mice. Bone marrow transplantation revealed that loss of RIP3 expression from bone-marrow-derived cells is responsible for the reduced disease progression. While no difference was found in apoptosis between *RIP3*$^{-/-}$;*Ldlr*$^{-/-}$ and *RIP3*$^{+/+}$;*Ldlr*$^{-/-}$ mice, electron microscopy revealed a significant reduction of macrophage primary necrosis in the advanced lesions of *RIP3*$^{-/-}$ mice. In vitro cellular studies showed that *RIP3* deletion had no effect on oxidized low-density lipoprotein (LDL)-induced macrophage apoptosis, but prevented macrophage primary necrosis occurring in response to oxidized LDL under caspase inhibition or RIP3 overexpression conditions. RIP3-dependent necrosis is not postapoptotic, and the increased primary necrosis in advanced atherosclerotic lesions most likely resulted from the increase of RIP3 expression. Our data demonstrate that primary necrosis of macrophages is proatherogenic during advanced atherosclerosis development.

INTRODUCTION

Macrophages have been well known to play a key role in atherosclerosis development (Moore and Tabas, 2011; Tabas, 2010). During the initial stages of atherosclerosis, blood-borne monocytes are recruited into the subendothelial space of the blood vessel and differentiate into macrophages. Under nonresolving inflammatory conditions, monocytes continue to enter plaques and differentiate into macrophages as atherosclerotic lesions progress. Macrophages contribute to size-independent changes in plaque morphology, notably formation of the necrotic core and thinning of the fibrous cap, which characterize the "vulnerable" plaque (Moore and Tabas, 2011; Tabas, 2010). In response to lesional cytotoxic stimuli, macrophages usually undergo cell death. Apoptosis of macrophages has been studied in atherosclerosis development, which can either inhibit or promote the development of atherosclerosis, depending on the stage of atherogenesis (Tabas, 2010). In early lesions where efferocytosis is effective, macrophage apoptosis can thwart the progression of atherosclerosis. In contrast, when the clearance of apoptotic macrophages is ineffective in advanced lesions, the apoptotic macrophages are speculated to undergo postapoptotic necrosis and coalesce over time into a key feature of vulnerable plaques, the necrotic core. Necrotic core formation in these advanced atheromata is thought to promote plaque disruption and, ultimately, acute atherothrombotic vascular disease (Tabas, 2010).

Morphological analysis of human samples with a transmission electron microscope shows that there are signs of macrophage necrosis in atherosclerotic lesions (Bauriedel et al., 1998; Crisby et al., 1997; Hegyi et al., 1996). Perhaps due to the fact that necrosis has long been considered as an accidental and uncontrolled mode of cell death, atherosclerosis-associated necrotic death of macrophages has been believed to be mostly composed of postapoptotic events, though morphological analyses suggest the presence of primary necrosis in the lesions (Bauriedel et al., 1998; Crisby et al., 1997; Hegyi et al., 1996). One early study showed that prolonged free cholesterol loading can lead to macrophage necrosis; this in vitro phenomenon was proposed to be involved in macrophage necrosis in advanced atherosclerosis (Tabas et al., 1996). A recent study also showed that macrophages incubated with lipoproteins containing plant sterol can undergo death in a caspase-independent way with signs of necrosis and autophagy, which provides a possible mechanism for accelerated plaque necrosis in patients with sitosterolemia

(high levels of sitosterol and other plant sterol) (Bao et al., 2006). Those pioneering studies imply that primary necrosis of macrophage could play a role in atherosclerosis. However, to date there has not been any report to unambiguously address whether primary cellular necrosis occurs in atherosclerosis and whether it plays a role in plaque progression.

Recently, significant progress has been made in the study of programmed necrosis (also called necroptosis) (Han et al., 2011). A protein kinase, receptor interacting protein 3 (RIP3), was identified as a key regulator in mediating necrosis and switching apoptosis to necrosis (Cho et al., 2009; He et al., 2009; Zhang et al., 2009). Formation of necrosome complex containing RIP3, RIP1, caspase-8, and other proteins is essential for necrosis to proceed. Without RIP3, a similar signaling complex triggers apoptotic cell death. The intermodulation between apoptosis and necrosis is bidirectional, because caspase-8 also has an inhibitory effect on RIP3-mediated necrosis (Kaiser et al., 2011; Oberst et al., 2011). The necrosis and apoptosis pathways appear to compete with each other and can switch between each other depending on the balance between caspase-8 and RIP3 (Han et al., 2011). RIP3-dependent necrosis has now been shown to be a common cell-death pathway involved in cytokine-, virus-, and genotoxic stress-induced cell death and has also been demonstrated to be involved in a variety of pathological conditions, including the antiviral response (Cho et al., 2009), acute pancreatitis (He et al., 2009; Zhang et al., 2009), photoreceptor loss (Trichonas et al., 2010), embryonic lethality (Kaiser et al., 2011), and intestine inflammation (Welz et al., 2011).

In this study, we evaluated the role of RIP3-dependent necrosis in mouse models of atherosclerosis. We found that deletion of *RIP3* did not influence the development of early atherosclerosis, but significantly reduced the size of plaques in advanced atherosclerotic lesions. RIP3 has no role in macrophage apoptosis, but its deletion significantly reduced primary necrosis of macrophages in the lesions of advanced atherosclerosis. Necrotic macrophages are more difficult to remove through efferocytosis than apoptotic macrophages, and thus are more proinflammatory and proatherogenic. Our data suggest that increase of RIP3 expression in advanced atherosclerotic lesions promotes primary necrosis of macrophages, and demonstrates that RIP3-dependent necrosis plays an important role in the development of advanced atherosclerosis.

RESULTS

RIP3 Deficiency in Bone-Marrow-Derived Cells Reduces Advanced Atherosclerotic Lesions

Genetic deletion of *RIP3* in mice has no detectable effect in normal mouse development (Newton et al., 2004). Because of the essential role of RIP3 in necrotic cell death, *RIP3* knockout mice can be used to determine whether necrotic cell death plays any role in the development of atherosclerosis. To test the role of RIP3 in atherosclerosis, $RIP3^{-/-}$ mice were bred into atherosclerosis-prone $Ldlr^{-/-}$ and $Apoe^{-/-}$ backgrounds. The $RIP3^{+/+};Ldlr^{-/-}$ and $RIP3^{-/-};Ldlr^{-/-}$ mice were then fed a Western-type diet for either 8 or 16 weeks. Analysis of aortic lesion areas revealed no difference between the $RIP3^{+/+};Ldlr^{-/-}$ and $RIP3^{-/-};Ldlr^{-/-}$ mice fed with a Western-type diet for 8 weeks (Figure 1A), but there was a significant difference between $RIP3^{+/+};Ldlr^{-/-}$ and $RIP3^{-/-};Ldlr^{-/-}$ mice after the mice were fed a Western-type diet for 16 weeks ($p < 0.05$) (Figure 1B). It appears that RIP3 has little or no involvement in the early development of atherosclerosis, but has a promoting effect on advanced atherosclerosis.

Further analysis was performed for advanced atherosclerotic lesions at the aortic root. Quantitative analysis of representative images revealed that lesion areas were much smaller in $RIP3^{-/-};Ldlr^{-/-}$ mice compared with $RIP3^{+/+};Ldlr^{-/-}$ mice ($p < 0.05$) (Figure 1C). Analysis was also performed on features of the necrotic core, a key determinant of plaque vulnerability, which revealed a clear decrease in plaque necrosis in the $RIP3^{-/-}$ lesions. Quantification of this parameter for the entire cohort of mice indicated a 60% decrease in total necrotic areas in the lesions of $RIP3^{-/-};Ldlr^{-/-}$ mice ($p < 0.05$) (Figure 1D). In addition to plaque lesion areas and necrotic areas, other important "vulnerable plaque" features are disruption of collagen, fibrous cap thinning, and elastin depletion. Although no significant difference in elastin break numbers of plaque lesions was observed between 16 week Western-diet-fed $RIP3^{+/+};Ldlr^{-/-}$ and $RIP3^{-/-};Ldlr^{-/-}$ mice (Figure S1A), *RIP3* deficiency significantly reduces the degradation of collagen and thinning of the fibrous cap (Figures S1B and S1C). Collectively, these results together with the reduced lesion areas and necrotic areas in $RIP3^{-/-};Ldlr^{-/-}$ mice demonstrate that *RIP3* deficiency prevents atherosclerosis development.

To investigate the possible cell types involved, bone marrow transplantation was carried out with lethally irradiated female $RIP3^{+/+};Ldlr^{-/-}$ mice as recipients. Those mice were transplanted with bone marrow from either $RIP3^{+/+};Ldlr^{-/-}$ or $RIP3^{-/-};Ldlr^{-/-}$ mice. Mice transplanted with $RIP3^{-/-};Ldlr^{-/-}$ bone marrow showed less lesion areas than the mice transplanted with $RIP3^{+/+};Ldlr^{-/-}$ bone marrow after being fed with a Western-type diet for 16 weeks (Figure 2), suggesting that *RIP3* deficiency in macrophages plays a role in reducing atherosclerotic lesions. Since body weight and plasma lipid levels are associated with the development of atherosclerosis, we compared body weight and plasma lipid levels between $RIP3^{+/+};Ldlr^{-/-}$ and $RIP3^{-/-};Ldlr^{-/-}$ mice after being fat-fed for 16 weeks. As shown in Figure S1D, there was no difference between $RIP3^{+/+}$ and $RIP3^{-/-}$ groups in body weight, total cholesterol (TC), low-density lipoprotein cholesterol (LDLC), high-density lipoprotein cholesterol (HDLC), and triglyceride (TG).

$RIP3^{+/+};Apoe^{-/-}$ and $RIP3^{-/-};Apoe^{-/-}$ mice were also used to study the role of RIP3 in atherosclerosis and the results obtained were very similar: decreased aortic lesion areas, decreased atherosclerotic lesions, and necrotic areas at the aortic root in $RIP3^{-/-}$ mice (Figures S2A–S2C), and no difference in body weight, TC, LDLC, HDLC, and TG between $RIP3^{+/+}$ and $RIP3^{-/-}$ mice (Figure S2D).

RIP3 Deficiency Reduces Primary Necrosis of Macrophages in Advanced Atherosclerotic Lesions but Has No Effect on Macrophage Apoptosis

It is known that macrophage death plays a key role in atherosclerosis and that both apoptosis and necrosis of macrophages are

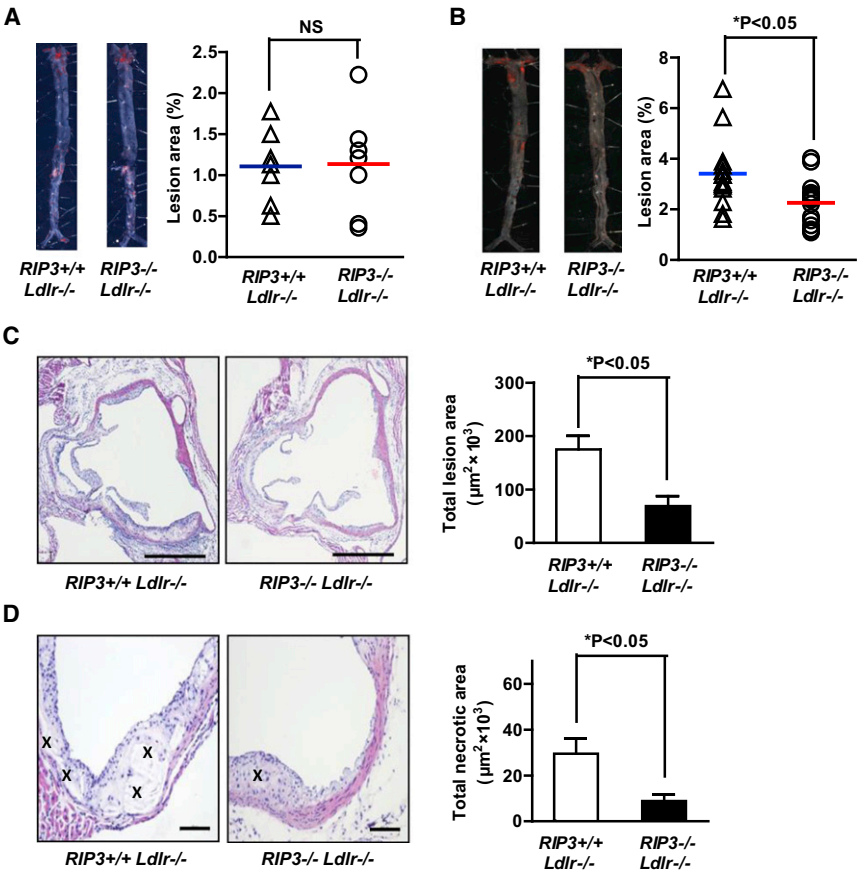

Figure 1. *RIP3*$^{-/-}$;*Ldlr*$^{-/-}$ Mice Have Reduced Lesion and Necrotic Area Compared to *RIP3*$^{+/+}$;*Ldlr*$^{-/-}$ Mice after Being Fed a Western-type Diet for 16 Weeks

(A) *RIP3*$^{+/+}$;*Ldlr*$^{-/-}$ (n = 7) and *RIP3*$^{-/-}$;*Ldlr*$^{-/-}$ (n = 7) female mice fed a Western-type diet for 8 weeks. Representative images of pinned Sudan-IV-stained aortas and quantification of the surface area occupied by the lesions (percent area occupied by the lesions) are shown. Horizontal lines within the data sets represent means. Each symbol represents a measurement from a single mouse. NS, no significant difference.

(B) *RIP3*$^{+/+}$;*Ldlr*$^{-/-}$ (n = 14) and *RIP3*$^{-/-}$;*Ldlr*$^{-/-}$ (n = 16) female mice fed a Western-type diet for 16 weeks. Representative images of pinned Sudan-IV-stained aortas and quantification of the surface area occupied by the lesions (percent area occupied by the lesions) are shown. Horizontal lines within the data sets represent means. Each symbol represents a measurement from a single mouse. *p < 0.05.

(C) The images show representative sections of aortic roots from the mice described in (B) stained with hematoxylin and eosin (H&E). Bar scales, 500 μm. Quantitative analyses of atherosclerotic lesion size in H&E-stained aortic root sections are shown. Data are expressed as mean ± SEM. *p < 0.05.

(D) Representative sections of H&E-stained aortic roots from each group (X indicates necrotic area). Bar scales, 100 μm. The bar graph shows quantification of anuclear, afibrotic, and eosin-negative necrotic areas. Data are expressed as mean ± SEM. *p < 0.05.

See also Figures S1 and S2.

present in atherosclerotic lesions (Bauriedel et al., 1998; Crisby et al., 1997; Hegyi et al., 1996; Moore and Tabas, 2011; Tabas, 2010). Because RIP3 is essential for cell necrosis and the bone marrow transplantation results suggest that *RIP3* deficiency in macrophages reduces lesion development (Figure 2), we sought to determine whether *RIP3* knockout has any effect on macrophage apoptosis or necrosis. Because macrophage apoptosis and necrosis in atherosclerotic plaques can be identified morphologically under a transmission electron microscope (Bauriedel et al., 1998; Crisby et al., 1997; Hegyi et al., 1996), apoptotic and necrotic macrophages within atherosclerotic intimal areas at the aortic roots from *RIP3*$^{+/+}$;*Ldlr*$^{-/-}$ mice and *RIP3*$^{-/-}$;*Ldlr*$^{-/-}$ mice were analyzed (Figure S3). Apoptotic macrophages in lesional intima are characterized by cell and nuclear shrinkage, chromatin condensation, and presence of apoptotic bodies, whereas necrotic macrophages show plasma membrane rupture with no apoptotic nuclear changes. Three pairs of 8-week fat-fed and four pairs of 16-week fat-fed *RIP3*$^{+/+}$;*Ldlr*$^{-/-}$ and *RIP3*$^{-/-}$;*Ldlr*$^{-/-}$ mice were used to measure macrophage apoptosis and necrosis. Atherosclerotic plaques of aortic roots from each mouse were analyzed using electron microscopy. As shown in the left panel of Figure 3A, macrophage death in 8-week fat-fed mice is predominantly apoptotic, and there is no difference between *RIP3*$^{+/+}$ and *RIP3*$^{-/-}$ mice in either apoptotic or necrotic macrophage death. In contrast, although the numbers of apoptotic macrophages in 16-week fat-fed *RIP3*$^{+/+}$ and *RIP3*$^{-/-}$ mice were similar, *RIP3* deletion was found to result in about a 50% decrease in necrotic macrophages in the atherosclerosis plaques (Figure 3A, right panel).

To further confirm that *RIP3* deficiency had no effect on macrophage apoptosis in the atherosclerotic lesions of 16-week fat-fed mice, activated caspase-3 was immunostained in serial sections from the proximal aorta, and no difference was found between *RIP3*$^{+/+}$;*Ldlr*$^{-/-}$ and *RIP3*$^{-/-}$;*Ldlr*$^{-/-}$ mice (Figure 3B) or between *RIP3*$^{+/+}$;*Apoe*$^{-/-}$ and *RIP3*$^{-/-}$;*Apoe*$^{-/-}$ mice (Figure S2E). Similarly, TUNEL staining of the lesions from *RIP3*$^{+/+}$;*Ldlr*$^{-/-}$ and *RIP3*$^{-/-}$;*Ldlr*$^{-/-}$ mice showed no difference between the two groups of mice (Figure 3C). Collectively, the data demonstrate that RIP3 does not play any role in macrophage apoptosis, but promotes macrophage necrosis in advanced lesions.

RIP3-Dependent Macrophage Necrosis Is Not a Postapoptotic Form of Cell Death

The correlation between reduced lesion sizes and decreased macrophage necrosis in *RIP3*-deficient mice suggests that RIP3-dependent macrophage necrosis may promote the development of advanced atherosclerosis. Therefore, in vitro experiments were carried out to further characterize the feature of RIP3-dependent macrophage death. Translocation of

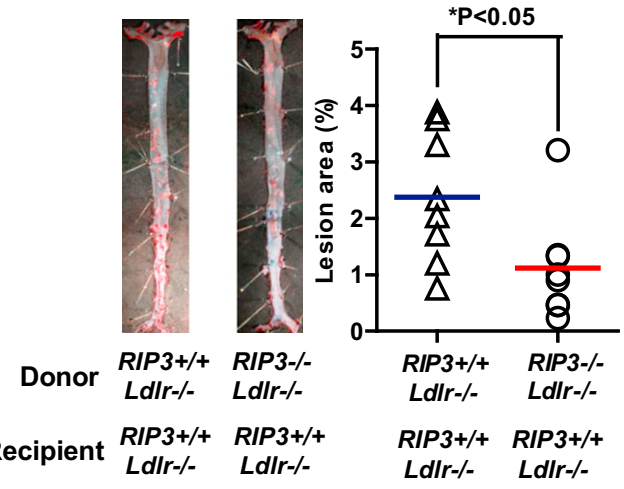

Figure 2. Lethally Irradiated *RIP3*$^{+/+}$;*Ldlr*$^{-/-}$ Mice Transplanted with *RIP3*$^{-/-}$;*Ldlr*$^{-/-}$ Bone Marrow Have Reduced Lesion Area as Compared with mice Transplanted with *RIP3*$^{+/+}$;*Ldlr*$^{-/-}$ Bone Marrow

Eight-week-old female *RIP3*$^{+/+}$;*Ldlr*$^{-/-}$ mice were lethally irradiated and transplanted with female *RIP3*$^{+/+}$;*Ldlr*$^{-/-}$ (n = 8) or *RIP3*$^{-/-}$;*Ldlr*$^{-/-}$ (n = 8) bone marrow. Eight weeks posttransplantation, the two groups were fed with a Western diet for 16 weeks. Representative images of pinned Sudan-IV-stained aortas and quantifications of the surface areas occupied by the lesions (percent area occupied by the lesions) are shown. Horizontal lines within the data sets represent means. Each symbol represents a measurement from a single mouse. *p < 0.05.

phosphatidylserine from the inner part of the plasma membrane to the outer layer is an early event in apoptosis, which can be detected by annexin V staining. Treatment of *RIP3*$^{+/+}$ and *RIP3*$^{-/-}$ macrophages with oxidized low-density lipoprotein (oxLDL) for 12 hr led to the appearance of about 10% annexin V-positive cells in both *RIP3*$^{+/+}$ and *RIP3*$^{-/-}$ cells (Figure 4A, upper panel). Uptake of propidium iodide (PI) is an indicator of a loss in cell-membrane integrity. The 12 hr oxLDL treatment did not lead to the appearance of detectable PI-positive cells in either *RIP3*$^{+/+}$ or *RIP3*$^{-/-}$ macrophages (Figure 4A, lower panel). The annexin V-positive and PI-negative cells should be apoptotic cells. These data indicated that oxLDL induces macrophage apoptosis and that RIP3 is not involved in oxLDL-induced apoptosis of macrophages. Similarly, it was found that *RIP3* deficiency did not have any effect on macrophage apoptosis induced by other proatherogenic apoptotic stimuli (data not shown), including 7-KC, 25-HOC, and oxLDL plus SIN-1, which generates peroxynitrite and induces endoplasmic reticulum stress in cells (Thorp et al., 2009).

Because inhibition of caspases in fibroblasts and other cells blocks apoptosis and simultaneously enhances RIP3-dependent necrosis (Zhang et al., 2009), the possible effect of caspase inhibition on oxLDL-induced macrophage death was evaluated. Treatment of macrophages with pan-caspase inhibitor zVAD alone had no effect on cell viability (Figure 4A). zVAD did not reduce but rather dramatically increased oxLDL-induced annexin V-positive cells in *RIP3*$^{+/+}$ macrophages (Figure 4A, upper panel). These annexin V-positive cells were different from those with oxLDL treatment alone, because they were also PI positive (Figure 4A, lower panel), indicating that oxLDL-induced macrophage necrosis occurred under caspase inhibition. Electron microscopy analysis revealed a dramatic increase in macrophage death with the morphology of primary necrosis (Figure 4B). In addition, rapid loss of plasma membrane integrity was also detected through the release of radiolabeled materials from the cells (Figure 4C) in *RIP3*$^{+/+}$ macrophages treated with oxLDL in the presence of zVAD. Therefore, caspase inhibition switches oxLDL-induced macrophage death from apoptosis to necrosis. Notably, necrotic cell death was completely abolished in RIP3-deficient macrophages (Figures 4A–4C). Similarly, caspase inhibition also enhanced RIP3-dependent macrophage necrosis induced by 7-KC and 25-HOC (data not shown).

Because necrotic cell death could be a postapoptotic event, we next examined the dynamic relationship between oxLDL-induced apoptosis and RIP3-dependent necrosis. Sixty hours of oxLDL treatment caused 100% of cells to become annexin V positive (Figure 4D, upper panel). PI-positive cells were barely detectable before 60 hr, but appeared at a later time (Figure 4D, upper panel). These PI-positive cells most likely resulted from postapoptotic necrosis. There was no difference between *RIP3*$^{+/+}$ and *RIP3*$^{-/-}$ macrophages in oxLDL-induced apoptosis and postapoptotic necrosis (Figure 4D, upper panel). We then analyzed the time course of cell death in oxLDL-plus-zVAD-treated macrophages. OxLDL plus zVAD led to quick death of *RIP3*$^{+/+}$ macrophages with a necrotic phenotype of annexin V and PI double-positive staining (Figure 4D, lower panel). This type of cell death depends on RIP3 because it was blocked when *RIP3* was deleted in macrophages (Figure 4D, lower panel). To confirm that oxLDL-plus-zVAD-induced macrophage death is necrosis, active caspase-3 was stained and TUNEL assay was used to determine whether these apoptosis markers were absent in oxLDL-plus-zVAD-treated macrophages. Sixteen hours of oxLDL plus zVAD treatment resulted in annexin V and PI double-positive staining in almost all *RIP3*$^{+/+}$ macrophages, but not *RIP3*$^{-/-}$ cells (Figures S4Ac and S4Ad). No caspase-3 activation or TUNEL-positive signals were detected in these cells (Figures S4Bc and S4Cc), indicating that those cells did not undergo apoptosis. In contrast, caspase-3 activation and TUNEL-positive signals were detected in both *RIP3*$^{+/+}$ and *RIP3*$^{-/-}$ macrophages treated solely with oxLDL for 72 hr (Figures S4Ae, S4Af, S4Be, S4Bf, S4Ce, and S4Cf), indicating that oxLDL-induced cell death is apoptosis. Collectively, these data demonstrate that RIP3 is not involved in apoptosis or postapoptotic necrosis, but rather plays a key role in the primary necrosis of macrophages. These in vitro data are consistent with the data obtained by analyzing atherosclerotic lesions, which showed a decrease in macrophage primary necrosis in *RIP3*$^{-/-}$ mice (Figure 3A).

RIP3 Deficiency Reduces Lesional Inflammation and Macrophage Infiltration in Advanced Lesions

Because inflammation in lesions plays an important role in the acceleration of atherosclerosis (Barish et al., 2008; Lee et al., 2003; Moore and Tabas, 2011; Tabas, 2010), we tested whether *RIP3* deficiency affects the inflammatory responses or the efferocytosis of macrophages, both of which can regulate

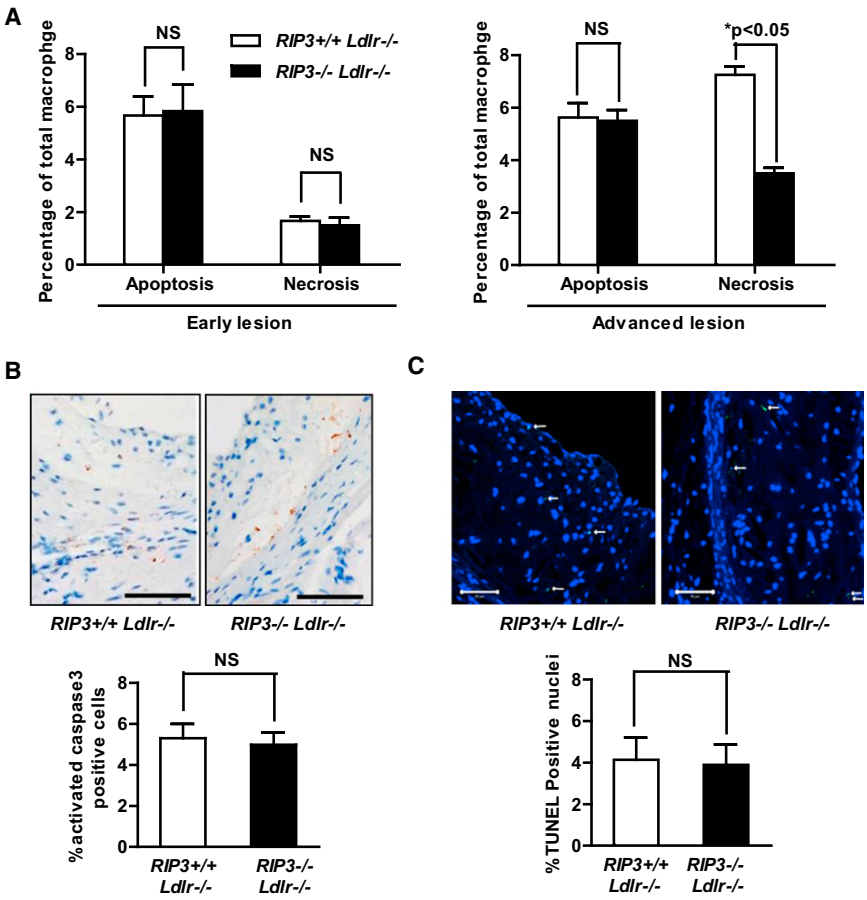

Figure 3. Advanced Lesions of *RIP3*$^{-/-}$;*Ldlr*$^{-/-}$ Mice Have Reduced Macrophage Necrosis as Compared to *RIP3*$^{+/+}$;*Ldlr*$^{-/-}$ Mice

(A) Statistics of apoptotic and necrotic macrophages within intimal area from early and advanced lesions at mouse aortic roots. A total of 200 macrophages within the lesional intima were counted, and quantifications of apoptotic and necrotic macrophage percentages are shown for *RIP3*$^{+/+}$;*Ldlr*$^{-/-}$ and *RIP3*$^{-/-}$;*Ldlr*$^{-/-}$ mice after an 8-week (early lesion, three pairs, left panel) or a 16-week (advanced lesion, four pairs, right panel) Western diet. Data shown represent mean ± SEM. NS, no significant difference; *p < 0.05.

(B) Representative micrographs showing activated caspase-3 in aortic root lesions from *RIP3*$^{+/+}$;*Ldlr*$^{-/-}$ (n = 10) and *RIP3*$^{-/-}$;*Ldlr*$^{-/-}$ (n = 10) mice by immunohistochemistry. Bar scales: 50um. A quantitative analysis of aortic root lesional active caspase-3 positive cells for each group is shown. Data shown represent mean ± SEM. NS, no significant difference.

(C) Representative micrographs showing TUNEL positive cells in aortic root lesions from *RIP3*$^{+/+}$;*Ldlr*$^{-/-}$ and *RIP3*$^{-/-}$;*Ldlr*$^{-/-}$ mice by immunefluorescence. Bar scales, 100 μm. A quantitative analysis of aortic root lesional TUNEL positive cells for each group (n = 5) is shown. Data shown represent mean ± SEM. NS, no significant difference.

See also Figures S2 and S3.

inflammation in lesions. First, *RIP3*$^{+/+}$ and *RIP3*$^{-/-}$ peritoneal macrophages were treated with oxLDL and the expressions of a number of different cytokines and chemokines were measured; no differences were found between *RIP3*$^{+/+}$ and *RIP3*$^{-/-}$ cells in oxLDL-induced tumor necrosis factor (TNF), interleukin 1β, monocyte chemoattractant protein 1 (MCP1), MCP2, MCP3, macrophage inflammatory protein 1-α (MIP1α), MIP1β, or interferon gamma-induced protein 10 transcription (Figure S5A). This is consistent with a published study that showed that RIP3 does not regulate cytokine production (Newton et al., 2004). We next evaluated the efficiency of phagocytic clearance of dead cells (efferocytosis) by *RIP3*$^{+/+}$ and *RIP3*$^{-/-}$ macrophages. There was no difference in the ability of *RIP3*$^{+/+}$ versus *RIP3*$^{-/-}$ macrophages in engulfing oxLDL-induced apoptotic macrophages, regardless of whether the apoptotic cells were *RIP3*$^{+/+}$ or *RIP3*$^{-/-}$ (Figure S5B), or in engulfing oxLDL-plus-zVAD-induced necrotic macrophages (Figure S5B). It is important to note that necrotic macrophages are poorer substrate for phagocytes compared to apoptotic macrophages (Figure S5B), which is consistent with previous studies (Kono and Rock, 2008). The inefficient clearance of necrotic macrophages could aggravate the proinflammatory effect of RIP3-dependent macrophage necrosis in advanced atherosclerosis, because cellular necrosis can release damaging intracellular molecules into the extracellular milieu and stimulate inflammatory responses. To evaluate whether inflammatory responses are different between *RIP3*$^{+/+}$ and *RIP3*$^{-/-}$ mice at the onset of atherosclerosis development, total RNA from whole lesions of *RIP3*$^{+/+}$;*Ldlr*$^{-/-}$ and *RIP3*$^{-/-}$;*Ldlr*$^{-/-}$ mice in advanced stages was extracted, and the results showed that overall, the mRNA levels of the cytokines tested were slightly higher in *RIP3*$^{+/+}$;*Ldlr*$^{-/-}$ advanced lesions (Figure 5A). Statistically significant differences were observed in the mRNA levels of MIP1β, TNF, and vascular cell adhesion molecule 1 (VCAM-1). VCAM-1 expression by vascular cells is a characteristic feature of atherosclerosis, reflecting the inflammatory state in the plaque (Cybulsky and Gimbrone, 1991; Libby, 2002; Tupin et al., 2004). Similar to the lower VCAM-1 mRNA level in *RIP3*$^{-/-}$;*Ldlr*$^{-/-}$ advanced lesion, there was also reduction of VCAM-1 positive areas in *RIP3*$^{-/-}$;*Ldlr*$^{-/-}$ lesions (Figure 5B). Immunohistological detection of macrophages, using a Mac-2 antibody, showed greatly reduced staining in lesions at the aortic roots of *RIP3*$^{-/-}$;*Ldlr*$^{-/-}$ mice compared to those of *RIP3*$^{+/+}$;*Ldlr*$^{-/-}$ littermate mice (Figure 5C). A significant decrease in Mac-2-positive areas was also seen in *RIP3*$^{-/-}$;*Apoe*$^{-/-}$ mice compared to *RIP3*$^{+/+}$;*Apoe*$^{-/-}$ littermate mice (Figure S2F). These data indicate that reduced lesions in the absence of RIP3 are partially due to the decreased accumulation of macrophages in lesions, which are known to participate in a maladaptive, nonresolving inflammatory response that expands the subendothelial layer due to the

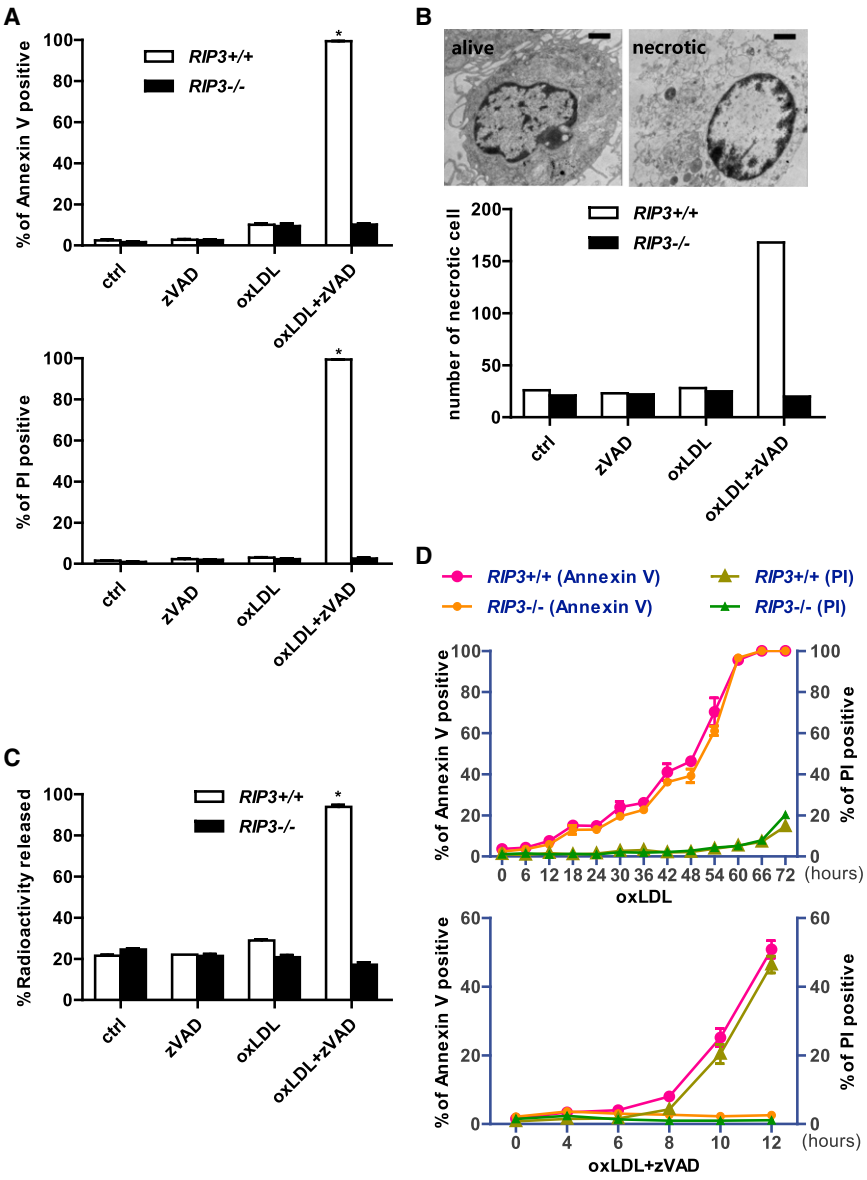

Figure 4. RIP3-Dependent Necrosis Is Not a Postapoptotic Cell Death

(A) Peritoneal macrophages from *RIP3*$^{+/+}$ and *RIP3*$^{-/-}$ mice were treated for 12 hr with vehicle control (DMSO), zVAD (20 μM), oxLDL (150 μg/ml), and oxLDL (150 μg/ml) plus zVAD (20 μM). Percentages of annexin V- or PI-positive macrophages are shown. Data are expressed as mean ± SEM.

(B) The *RIP3*$^{+/+}$ and *RIP3*$^{-/-}$ peritoneal macrophages were treated for 10 hr with vehicle control, zVAD, oxLDL, and oxLDL plus zVAD. Representative morphologies of alive and necrotic peritoneal macrophages are shown (upper panel). Scale bars, 1 μm. Among the 200 macrophages counted, the number of necrotic cells was recorded for each sample and is shown (lower panel).

(C) Peritoneal macrophages from *RIP3*$^{+/+}$ and *RIP3*$^{-/-}$ mice were loaded with [^{3}H]adenine for 2 hr and then treated with vehicle control, zVAD, oxLDL, and oxLDL plus zVAD. The supernatants were harvested and the cells were lysed; radioactivity was measured by scintillation counting, and the percentage of released radioactivity was calculated. Data are expressed as mean ± SEM.

(D) Peritoneal macrophages from *RIP3*$^{+/+}$ and *RIP3*$^{-/-}$ mice were loaded with oxLDL and oxLDL plus zVAD for the time indicated. Quantification of annexin V- or PI-positive macrophage percentages at each time point is shown. Data are expressed as mean ± SEM.

See also Figure S4.

infiltration of macrophages and accumulation of lipid and matrix (Moore and Tabas, 2011).

Caspase-8 Inhibition or RIP3 Upregulation Sensitize Macrophages to oxLDL-Induced Necrosis

Studies from our and other laboratories have demonstrated that caspase-8-dependent apoptosis and RIP3-dependent necrosis compete with each other in mediating cell death (Han et al., 2011; Kaiser et al., 2011; Oberst et al., 2011). Increased expression of RIP3 can convert cell death from apoptosis to necrosis (Zhang et al., 2009). On the other hand, a complex of caspase-8 and $FLIP_L$, in which caspase-8 is not processed but retains protease activity, can prevent RIP3 from mediating necrosis (Oberst et al., 2011). The data in Figure 4 already showed cross-inhibition between apoptosis and necrosis in oxLDL-treated macrophages, because inhibition of caspases promotes RIP3-dependent necrosis. To determine which caspase(s) plays a key role in blocking oxLDL-induced macrophage necrosis, we tested different caspase inhibitors. Cell necrosis was determined by Annexin V/PI double staining (Figure 6A). Another pan-caspase inhibitor similar to zVAD, QVD, also enhanced oxLDL-induced macrophage necrosis. Caspase-8-specific inhibitor IETD, but neither caspase-3 inhibitor DEVD nor caspase-1 inhibitor WEHD, promoted oxLDL-induced macrophage necrosis. Thus, inhibition of caspase-8 plays a major role in promoting oxLDL-induced macrophage necrosis.

Next, whether increasing RIP3 activity by overexpression of RIP3 in macrophages can convert apoptosis to necrosis was examined. Indeed, oxLDL alone triggered necrosis in macrophage cell line Raw 264.7 by overexpressing RIP3 over a certain level (Figure 6B), similar to the reported conversion of apoptosis to necrosis by increased RIP3 expression in fibroblast and epithelial cell lines (Sun et al., 2012; Zhang et al., 2009). It is noteworthy that percentages of necrotic cells positively correlate with the RIP3 level in the macrophages.

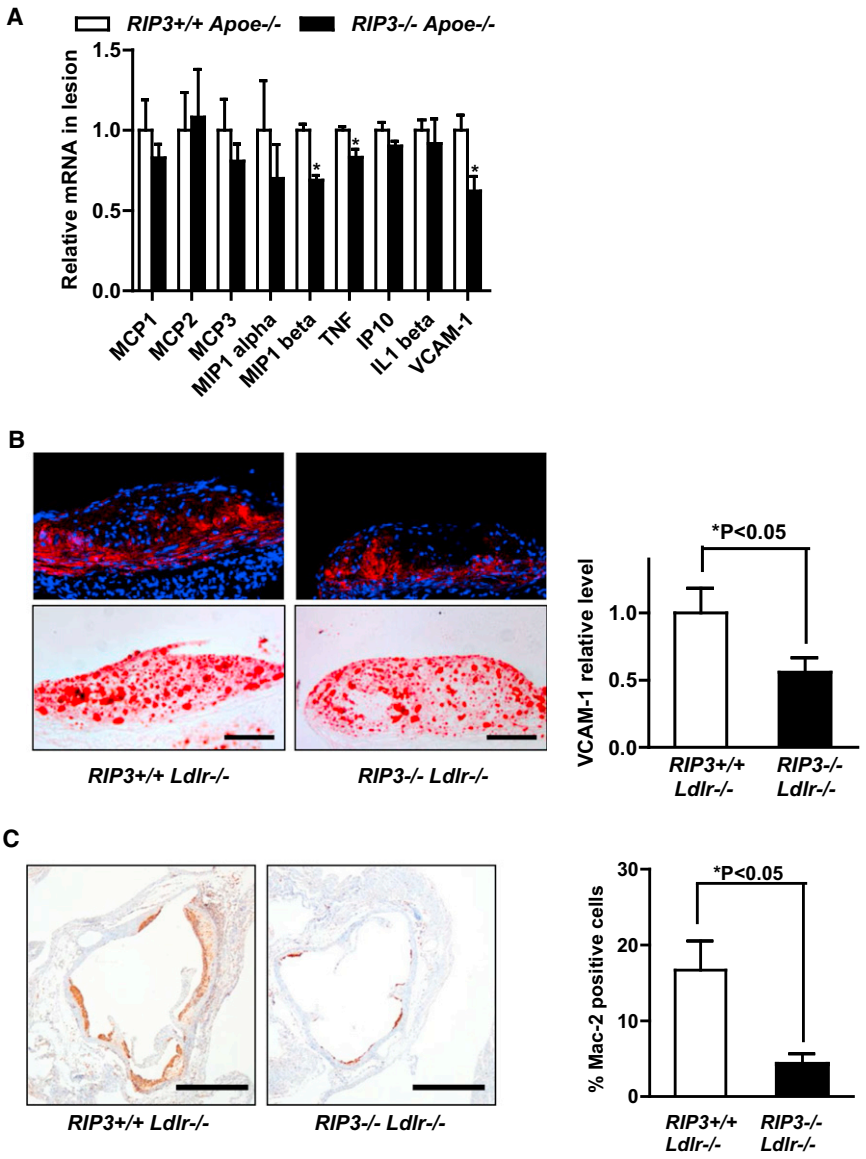

Figure 5. Less Inflammation and Macrophage Infiltration in the Advanced Lesions of *RIP3*$^{-/-}$;*Ldlr*$^{-/-}$ Mice

(A) Relative expression levels of cytokine and chemokine mRNA in lesions from 16-week fat-fed *RIP3*$^{+/+}$;*Ldlr*$^{-/-}$ and *RIP3*$^{-/-}$;*Ldlr*$^{-/-}$ mice were measured by quantitative RT-PCR. The gene expression levels were normalized to the expression of GAPDH. Data are presented as means ± SEM. *p < 0.05.

(B) Representative photographs of VCAM-1 expression in advanced lesions from aortic roots. Lesions developed in *RIP3*$^{+/+}$;*Ldlr*$^{-/-}$ or *RIP3*$^{-/-}$;*Ldlr*$^{-/-}$ mice after 16 weeks on a Western diet were stained for VCAM-1 (upper; red signal is VCAM-1 positive, blue signal is DAPI) and Oil Red O (lower). Bar scale, 100 μm. A quantitative analysis of VCAM-1 expression at aortic root lesions in four pairs of *RIP3*$^{+/+}$;*Ldlr*$^{-/-}$ and *RIP3*$^{-/-}$;*Ldlr*$^{-/-}$ mice is shown. The mean value of VCAM-1-positive areas from the four *RIP3*$^{+/+}$;*Ldlr*$^{-/-}$ mice was set as 1. Data are expressed as mean ± SEM. *p < 0.05.

(C) Representative micrographs show Mac-2-positive cells in aortic root lesions from *RIP3*$^{+/+}$;*Ldlr*$^{-/-}$ *and RIP3*$^{-/-}$;*Ldlr*$^{-/-}$ mice by immunohistochemical staining. A quantitative analysis of aortic root lesional macrophage infiltration in *RIP3*$^{+/+}$;*Ldlr*$^{-/-}$ (n = 5) and *RIP3*$^{-/-}$;*Ldlr*$^{-/-}$ (n = 7) mice is shown. Scale bars, 500 μm. Data are expressed as mean ± SEM. *p < 0.05.

See also Figure S5.

RIP3 Upregulation in Lesional Macrophages during Lesion Development Induces Macrophage Necrosis and Promotes Lesion Development

We then speculated that RIP3-dependent necrosis of macrophages in advanced atherosclerotic lesions resulted from either increased RIP3 expression or reduced caspase-8 expression. To evaluate this hypothesis, the levels of RIP3 and active or full-length caspase-8 in early and advanced lesions were examined. No difference was detected in active caspase-8 or full-length caspase-8 between early and advanced lesions from either *RIP3*$^{+/+}$;*Ldlr*$^{-/-}$ or *RIP3*$^{-/-}$;*Ldlr*$^{-/-}$ mice by western blotting (Figure S5C) However, the RIP3 level is higher in advanced lesions compared to early lesions in *RIP3.*$^{+/+}$;*Ldlr*$^{-/-}$ mice (Figure S5C).

To demonstrate that the RIP3 level is increased in macrophages in advanced lesions, laser capture microdissection was carried out to isolate smooth muscle cells and macrophages and to determine their RIP3 mRNA levels (Figure S6). It was found that although RIP3 level did not change between nonlesional smooth muscle cells and lesional smooth muscle cells (Figure 7A), its level in lesional macrophages increased as the lesion developed from a small size to large size (Figure 7B). Because cell-based experiments showed that the RIP3 level should exceed a certain threshold in order to induce cellular necrosis (Figure 6B), it is very likely that the RIP3 level in lesional macrophages should also exceed a certain threshold in order to induce necrosis. The importance of RIP3 expression level in determining the mode of cell death in vivo is supported by the comparison of lesion areas in *RIP3*$^{+/+}$;*Apoe*$^{-/-}$, *RIP3*$^{+/-}$;*Apoe* $^{-/-}$, and *RIP3*$^{+/-}$;*Apoe* $^{-/-}$ mice. It was found that *RIP3*$^{+/-}$;*Apoe* $^{-/-}$ mice had less lesion areas compared to *RIP3*$^{+/+}$; *Apoe* $^{-/-}$ mice, but more lesion areas compared to *RIP3*$^{-/-}$;*Apoe* $^{-/-}$ mice (Figure 7C). Thus, RIP3-mediated macrophage necrosis in advanced lesions most likely can be attributed to the increase of RIP3 expression in macrophages during the development of atherosclerosis.

DISCUSSION

Both apoptotic and necrotic macrophages were detected in atherosclerotic lesions from human patients and model animals.

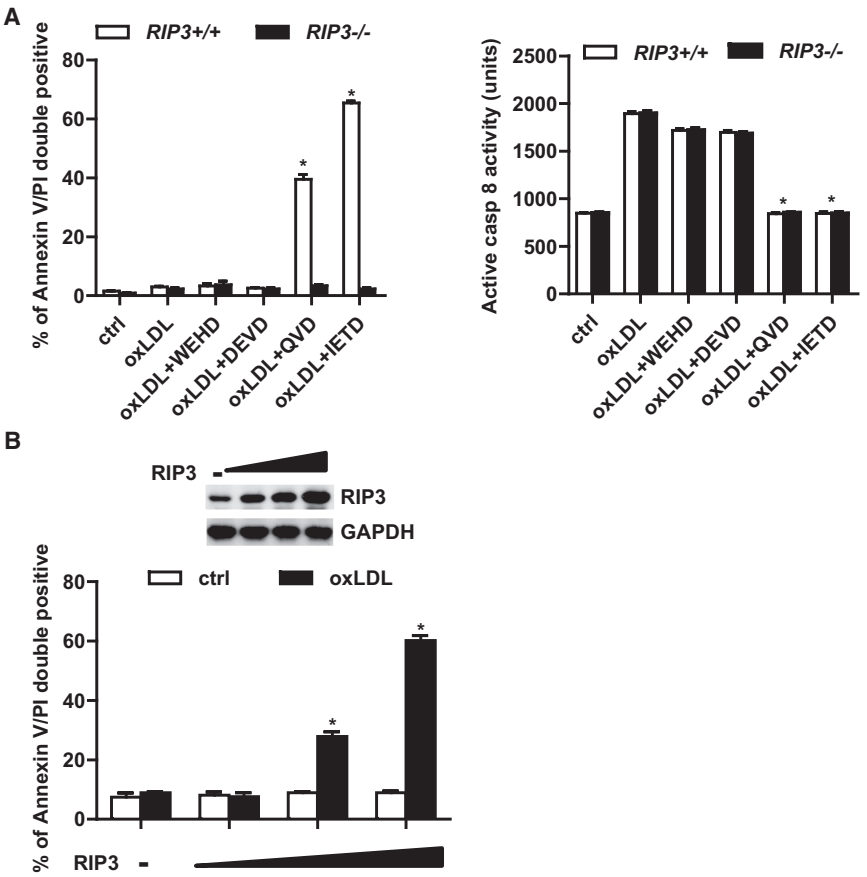

Figure 6. Caspase-8 Inhibition or RIP3 Overexpression Exceeding a Certain Threshold Switches oxLDL-Induced Apoptosis to Necrosis

(A) *RIP3*$^{+/+}$ and *RIP3*$^{-/-}$ peritoneal macrophages were treated for 12 hr with vehicle control, oxLDL, oxLDL plus DEVD (caspase-3 inhibitor), oxLDL plus WEHD (caspase-1 inhibitor), oxLDL plus QVD (pan caspase inhibitor), and oxLDL plus IETD (caspase-8 inhibitor), and then were analyzed by annexin V and PI staining. Percentage of annexin V and PI double-positive macrophages is shown (left panel). Data are expressed as mean ± SEM. *$p < 0.05$. Inhibition of caspase-8 by IETD and QVD is shown in the right panel.

(B) Raw 264.7 cells were infected with different doses of a RIP3-expressing lentivirus or an empty vector. The cells were then treated with or without oxLDL for 48 hr. Percentage of annexin V and PI double-positive cells is shown. Data are expressed as mean ± SEM. NS, no significant difference. *$p < 0.05$. RIP3 expression level was determined by western blot with an anti-RIP3 antibody.

See also Figure S5.

While the role of apoptosis in the development of atherosclerosis has been well studied, the involvement of necrosis has never been experimentally evaluated. Because of the limitation in our understanding toward the mechanisms of cellular necrosis, only postapoptotic cell disruption, termed secondary or postapoptotic necrosis, was considered in the formation of necrotic core in the lesions. Because of very recent advances in defining the mechanisms of programmed necrosis, we used *RIP3* knockout mice to address whether RIP3-dependent necrosis is involved in atherosclerosis. We found that RIP3-dependent macrophage death is primary necrosis and is not important in the early stages of the disease, but plays an important role in advanced atherosclerosis. RIP3-dependent necrosis accounts for half of the necrotic cells in advanced lesions, while the other half could be postapoptotic cells or primary necrosis controlled by yet unknown mechanisms. It appears that the conversion of macrophage apoptosis to RIP3-dependent necrosis occurs during the development of atherosclerosis toward the advanced stage. The underlying mechanism of this conversion most likely is the upregulation of RIP3 expression in lesional macrophages toward the later stages of the disease. Given the fact that necrotic cells are more difficult to clear than apoptotic cells, primary necrosis of macrophages in advanced lesions may not only be involved in plaque formation, but also cause more inflammatory cell infiltration, and thus have a strong proinflammatory and proatherogenic role.

The necrotic morphology of RIP3-dependent macrophage death was determined by electron microscope analysis (Figure 4B). Although these necrotic macrophages are annexin V/PI double positive as determined by cellular assays (Figures 4A, 4D, and S4A), they lack apoptotic markers such as active caspase-3 or TUNEL-positive signals (Figures S4B and S4C). The annexin V-positive staining of necrotic cells could have resulted from loss of integrity of the plasma membrane, which allows annexin V to interact with the phosphatidylserine located in the inner part of the plasma membrane. This also explains why inhibition of caspases by zVAD had no effect on annexin V staining in oxLDL-treated cells. Reactive oxygen species (ROS) derived from mitochondria has been proven to play a crucial role in the execution of RIP3-dependent necrosis (Zhang et al., 2009). We and others have revealed that RIP1 and RIP3 are required for mitochondrial ROS production in some cell lines during necrosis (Zhang et al., 2009). Similarly, the ROS scavenger butylated hydroxyanisole (BHA) and the RIP1 inhibitor Nec-1 (necrostatin-1) also effectively blocked RIP3-mediated necrosis and ROS production in oxLDL-plus-zVAD-treated *RIP3*$^{+/+}$ macrophages (data not shown), as did the inhibitor of glycolysis (2-DG), and inhibitors of the complexes of the electron transport chain (Amytal, TTFA, antimycin A, NaN3) (data not shown). Inhibitors of ATP synthase (oligomycin) and lactate dehydrogenase (oxamate) had no effect on oxLDL-plus-zVAD-induced necrosis and ROS production (data not shown). Therefore, oxLDL-plus-zVAD-induced RIP3-mediated macrophage necrosis is dependent on RIP1 kinase activity and mitochondrial ROS production. Similarly, the enhanced

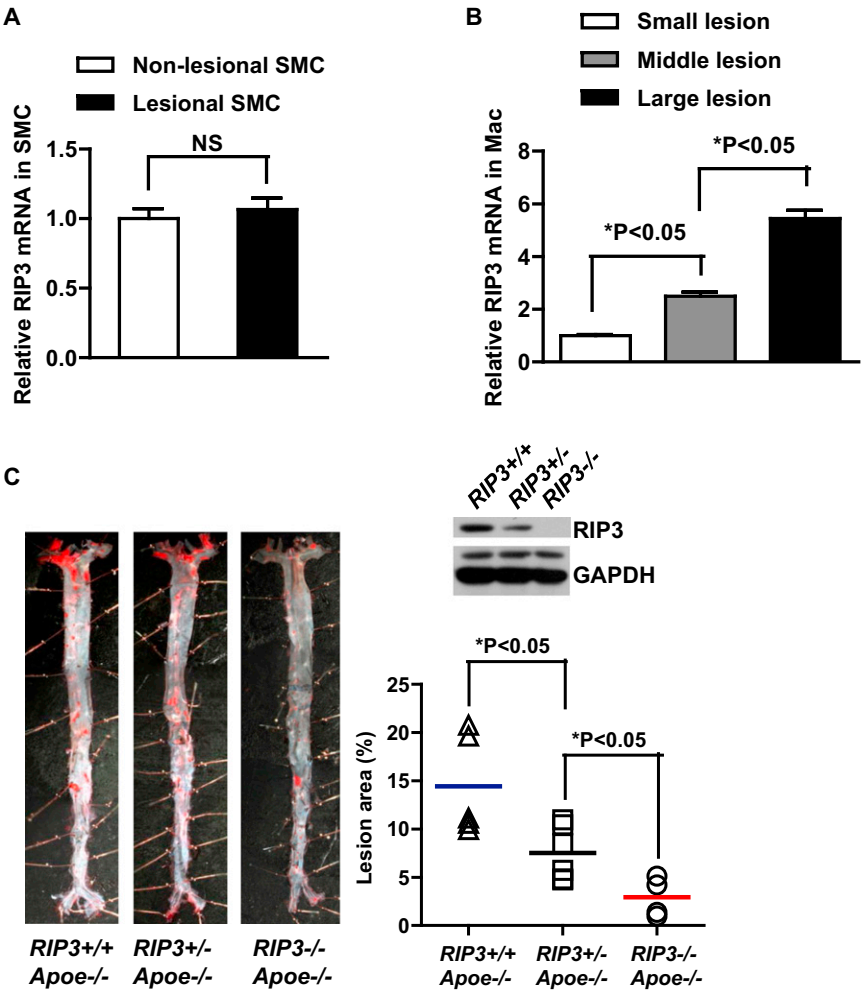

Figure 7. Increased RIP3 Expression during Lesion Development and the Correlation between In Vivo RIP3 Level and the Severity of Atherosclerotic Lesions

(A) RIP3 mRNA levels were compared between nonlesional SMC and lesional SMC isolated by laser capture microdissection from atherosclerotic lesions of 16-week fat-fed *RIP3*$^{+/+}$;*Ldlr*$^{-/-}$ mice. Data are presented as mean ± SEM. NS, no significant difference.

(B) RIP3 mRNA levels in lesional macrophages were compared among atherosclerotic lesions of different sizes (small, middle, and large). Data are expressed as mean ± SEM. *p < 0.05.

(C) Eight-week-old *RIP3*$^{+/+}$;*Apoe*$^{-/-}$ (n = 5), *RIP3*$^{+/-}$;*Apoe*$^{-/-}$ (n = 6), and *RIP3*$^{-/-}$;*Apoe*$^{-/-}$ (n = 4) mice were fed with a Western diet for 16 weeks. Representative images of pinned Sudan-IV-stained aortas and quantification of the surface area occupied by the lesions (percent area occupied by the lesions) are shown. Horizontal lines within the data sets represent means. Each symbol represents a measurement from a single mouse. *p < 0.05.

See also Figures S5 and S6.

oxLDL-induced cell death in the presence of QVD or IETD can also be inhibited by Nec-1 (data not shown). As anticipated, BHA, Nec-1, and inhibitors of glycolysis and the electron transport chain could not inhibit oxLDL-induced apoptosis in either *RIP3*$^{+/+}$ or *RIP3*$^{-/-}$ macrophages (data not shown). It is clear that macrophage necrosis uses the same execution pathway as the necrosis observed in other cell types, excepting extracellular stimuli. The cellular receptor/sensor(s) of oxLDL or other lipids that initiate the signaling linking to the RIP3-dependent necrosis pathway is currently unclear.

It has been well established that macrophage apoptosis occurs in atherosclerotic lesions, and stimuli (including oxLDL, 7-KC, 25-HOC, free cholesterol, etc.) that are thought to be proatherogenic also induce macrophage apoptosis in vitro. We found that these proapoptotic stimuli could be pronecrotic under conditions of caspase inhibition or RIP3 induction. Because caspase-8-dependent apoptosis and RIP3-dependent necrosis compete with each other in mediating cell death, the relative level of the two central mediators of cell death might determine the cell death mode responding to different upstream signals. An increase of RIP3 in advanced lesional macrophages was detected, but which atherosclerosis-related factors can induce RIP3 expression is currently unknown. Given the complicated in vivo situation for the development of atherosclerosis, it is possible that multiple factors are involved. Although our data suggest that the increase of RIP3 expression converts macrophage apoptosis to necrosis in advanced lesions, we cannot exclude other mechanisms, such as increasing RIP3 activity by eliminating RIP3 phosphatase and expression of caspase-8 inhibitor, that can modulate the balance between RIP3 and caspase-8 and thus are involved in the regulation of macrophage necrosis in advanced atherosclerosis. Nevertheless, the balance between RIP3 and caspase-8 should be a determinant of whether the cells undergo necrosis or apoptosis.

In short, the correlation between decreased macrophage primary necrosis in advanced lesions and improved disease condition in *RIP3*$^{-/-}$ mice demonstrates the contribution of RIP3-dependent macrophage necrosis in the development of atherosclerosis toward advanced stage. Although postapoptotic necrosis is well accepted to play a role in atherosclerosis development, the data reported here demonstrate a previously unidentified primary necrosis that plays an essential role in the development of advanced atherosclerosis. RIP3-mediated primary necrosis of macrophages could contribute to lesion development by directly coalescing into the necrotic core and secondarily exacerbating the maladaptive inflammatory response, thus promoting advanced atherosclerotic lesions. Interventions by the RIP3 signaling pathway may be used to modulate the development of atherosclerosis.

EXPERIMENTAL PROCEDURES

Mice and Diets

Mice were housed in a specific pathogen-free environment. All experiments were conducted in compliance with the regulations of Xiamen University. *RIP3*$^{-/-}$ mice from the C57BL6/J background were bred onto the *Ldlr*$^{-/-}$ and *Apoe*$^{-/-}$ C57BL6/J backgrounds to generate *RIP3*$^{+/-}$;*Apoe*$^{-/-}$ and *RIP3*$^{+/-}$;*Ldlr*$^{-/-}$ breeding pairs. Starting at 8 weeks of age, female progeny (*RIP3*$^{+/+}$;*Ldlr*$^{-/-}$ and *RIP3*$^{-/-}$;*Ldlr*$^{-/-}$ or *RIP3*$^{+/+}$;*Apoe*$^{-/-}$ and *RIP3*$^{-/-}$;*Apoe*$^{-/-}$) from these breeding pairs were fed a high-cholesterol Western-type diet for either 12 weeks (*Apoe*$^{-/-}$ study) or 16 weeks (*Ldlr*$^{-/-}$ study). For studying early lesions, female *RIP3*$^{+/+}$;*Ldlr*$^{-/-}$ and *RIP3*$^{-/-}$;*Ldlr*$^{-/-}$ mice were fed a Western-type diet for 8 weeks. The Western diet was produced by Vital River Laboratories (Beijing, China) according to the Formula from Harlan (TD.88137).

Oxidized Low-Density Lipoprotein

oxLDL was purchased from Unionbiol (Beijing, China). LDL was isolated from human plasma (density: 1.03–1.50; purity: 98%). Oxidized LDL was obtained by oxidizing LDL with copper sulfate.

Peritoneal Macrophages

Thioglycollate-elicited macrophages were obtained from 8-week-old *RIP3*$^{+/+}$;*Ldlr*$^{-/-}$, *RIP3*$^{-/-}$;*Ldlr*$^{-/-}$, *RIP3*$^{+/+}$, and *RIP3*$^{-/-}$ mice using a method described previously (Osuga et al., 2000). Because it was found that having a *Ldlr*$^{-/-}$ background did not affect the macrophages' response to the treatment of oxLDL or oxLDL plus zVAD, *RIP3*$^{+/+}$ and *RIP3*$^{-/-}$ macrophages were used in most of our experiments. The cells were resuspended in Dulbecco's modified Eagle medium containing 10% fetal calf serum (FCS), and 8 × 10^5 cells were plated in one well of a 48-well plate and cultured in 37°C, 5% CO_2 conditions.

Atherosclerotic Lesion Analysis

Mice were euthanized and their hearts and aortas were isolated. The degree of atherosclerosis was assessed by determining lesion sizes on both pinned-open aortas and serial cross-sections through the aortic root as modified from previous studies (Seimon et al., 2009; Sekiya et al., 2009; Thorp et al., 2009). The aorta was opened longitudinally along the ventral midline from the iliac arteries to the aortic root. After branching vessels were removed, the aorta was pinned out flat on a black wax surface. The lesions were treated with 70% ethanol and then stained with Sudan IV for 15 min, destained with 80% ethanol, and then washed with PBS. Aortic images were analyzed with Adobe Photoshop software, data are reported as the percentage of the aortic surface covered by lesions.

The hearts were perfused with saline containing 4% paraformaldehyde and fixed for more than 48 hr in the same solution. The basal halves of the hearts were embedded in Tissue-Tek OCT compound (or paraffin), and serial sections (~6 μm thick) were captured using a Cryostat microtome (Leica, Germany) or Paraffin microtome (Leica, Germany). As described in a previous study (Seimon et al., 2009), for morphometric lesion analysis, sections were stained with Harris hematoxylin and eosin (H&E). Total intimal lesion area (from internal elastic lamina to the lumen) and acellular/anuclear areas (negative for hematoxylin-positive nuclei) per cross-section were quantified by taking the average of six sections spaced 28 μm apart beginning at the base of the aortic root. The necrotic core was defined as a clear area that was H&E free. Boundary lines were drawn around these regions, and the area measurements were obtained by image analysis software. Lipids in lesion areas were stained with 0.5% Oil Red O (Sangon Biotech, Shanghai, China) in propylene glycol for 10 min at 60°C. Morphological analysis of collagen contents in the lesional area and of fibrous cap thickness was performed with a Masson trichrome stain kit (Maixin-Bio, Liaoning, China), whereas elastin breaks were conducted by an elastin stain kit (Maixin-Bio). Fibrous cap thickness was quantified by choosing the largest necrotic core from duplicate sections and measuring the thickness of the thinnest part of the cap. Analysis was performed by two independent experienced morphologists blinded to the genotype.

In Vitro Peritoneal Macrophage Cell Death Assay

Macrophage cell death was measured by annexin V-EGFP and PI staining as previously described (Feng et al., 2003). Macrophages were stained with annexin V-EGFP in annexin V binding buffer on ice for 20 min in the dark. The annexin V labeling solution was then removed; and PI labeling solution was added. Cells were immediately viewed with a 20× objective using an Olympus IX-70 inverted fluorescence microscope equipped with filters appropriate for fluorescein and PI. Four fields of cells for each condition (more than 1,000 cells) were counted. The total number of cells was measured by counterstaining with DAPI. The data are expressed as the percentage of these cells per total cells counted. Percentages of green fluorescent protein-positive and PI-positive cells were counted separately.

Statistics

Absent error bars in graphs signify that SEM values were smaller than the graphic symbols. Comparison of mean values between groups was evaluated by the two-tailed Student's t test, Mann-Whitney U test, or ANOVA. A p value of less than 0.05 was considered significant.

For further details, please refer to Extended Experimental Procedures.

SUPPLEMENTAL INFORMATION

Supplemental Information includes Extended Experimental Procedures and six figures and can be found with this article online at http://dx.doi.org/10.1016/j.celrep.2012.12.012.

LICENSING INFORMATION

ACKNOWLEDGMENTS

We thank Ping Chen at the School of Life Sciences, Xiamen University for her help with electron microscopy analysis. We thank K. Newton and V.M. Dixit for RIP3$^{-/-}$ mice. This work was supported by 973 Program 2009CB522200, Natural Science Foundation of China grants 30830092, 30921005, 91029304, 81061160512, 863 program 2012AA02A201, and 111 project B12001.

Received: May 31, 2012
Revised: November 19, 2012
Accepted: December 18, 2012
Published: January 17, 2013

REFERENCES

Bao, L.P., Li, Y.K., Deng, S.X., Landry, D., and Tabas, I. (2006). Sitosterol-containing lipoproteins trigger free sterol-induced caspase-independent death in ACAT-competent macrophages. J. Biol. Chem. *281*, 33635–33649.

Barish, G.D., Atkins, A.R., Downes, M., Olson, P., Chong, L.W., Nelson, M., Zou, Y., Hwang, H., Kang, H., Curtiss, L., et al. (2008). PPARdelta regulates multiple proinflammatory pathways to suppress atherosclerosis. Proc. Natl. Acad. Sci. USA *105*, 4271–4276.

Bauriedel, G., Schluckebier, S., Hutter, R., Welsch, U., Kandolf, R., Lüderitz, B., and Prescott, M.F. (1998). Apoptosis in restenosis versus stable-angina atherosclerosis: implications for the pathogenesis of restenosis. Arterioscler. Thromb. Vasc. Biol. *18*, 1132–1139.

Cho, Y.S., Challa, S., Moquin, D., Genga, R., Ray, T.D., Guildford, M., and Chan, F.K. (2009). Phosphorylation-driven assembly of the RIP1-RIP3 complex regulates programmed necrosis and virus-induced inflammation. Cell *137*, 1112–1123.

Crisby, M., Kallin, B., Thyberg, J., Zhivotovsky, B., Orrenius, S., Kostulas, V., and Nilsson, J. (1997). Cell death in human atherosclerotic plaques involves both oncosis and apoptosis. Atherosclerosis *130*, 17–27.

Cybulsky, M.I., and Gimbrone, M.A., Jr. (1991). Endothelial expression of a mononuclear leukocyte adhesion molecule during atherogenesis. Science *251*, 788–791.

Feng, B., Yao, P.M., Li, Y., Devlin, C.M., Zhang, D., Harding, H.P., Sweeney, M., Rong, J.X., Kuriakose, G., Fisher, E.A., et al. (2003). The endoplasmic reticulum is the site of cholesterol-induced cytotoxicity in macrophages. Nat. Cell Biol. *5*, 781–792.

Han, J., Zhong, C.Q., and Zhang, D.W. (2011). Programmed necrosis: backup to and competitor with apoptosis in the immune system. Nat. Immunol. *12*, 1143–1149.

He, S., Wang, L., Miao, L., Wang, T., Du, F., Zhao, L., and Wang, X. (2009). Receptor interacting protein kinase-3 determines cellular necrotic response to TNF-alpha. Cell *137*, 1100–1111.

Hegyi, L., Skepper, J.N., Cary, N.R.B., and Mitchinson, M.J. (1996). Foam cell apoptosis and the development of the lipid core of human atherosclerosis. J. Pathol. *180*, 423–429.

Kaiser, W.J., Upton, J.W., Long, A.B., Livingston-Rosanoff, D., Daley-Bauer, L.P., Hakem, R., Caspary, T., and Mocarski, E.S. (2011). RIP3 mediates the embryonic lethality of caspase-8-deficient mice. Nature *471*, 368–372.

Kono, H., and Rock, K.L. (2008). How dying cells alert the immune system to danger. Nat. Rev. Immunol. *8*, 279–289.

Lee, C.H., Chawla, A., Urbiztondo, N., Liao, D., Boisvert, W.A., Evans, R.M., and Curtiss, L.K. (2003). Transcriptional repression of atherogenic inflammation: modulation by PPARdelta. Science *302*, 453–457.

Libby, P. (2002). Inflammation in atherosclerosis. Nature *420*, 868–874.

Moore, K.J., and Tabas, I. (2011). Macrophages in the pathogenesis of atherosclerosis. Cell *145*, 341–355.

Newton, K., Sun, X., and Dixit, V.M. (2004). Kinase RIP3 is dispensable for normal NF-kappa Bs, signaling by the B-cell and T-cell receptors, tumor necrosis factor receptor 1, and Toll-like receptors 2 and 4. Mol. Cell. Biol. *24*, 1464–1469.

Oberst, A., Dillon, C.P., Weinlich, R., McCormick, L.L., Fitzgerald, P., Pop, C., Hakem, R., Salvesen, G.S., and Green, D.R. (2011). Catalytic activity of the caspase-8-FLIP(L) complex inhibits RIPK3-dependent necrosis. Nature *471*, 363–367.

Osuga, J., Ishibashi, S., Oka, T., Yagyu, H., Tozawa, R., Fujimoto, A., Shionoiri, F., Yahagi, N., Kraemer, F.B., Tsutsumi, O., and Yamada, N. (2000). Targeted disruption of hormone-sensitive lipase results in male sterility and adipocyte hypertrophy, but not in obesity. Proc. Natl. Acad. Sci. USA *97*, 787–792.

Seimon, T.A., Wang, Y., Han, S., Senokuchi, T., Schrijvers, D.M., Kuriakose, G., Tall, A.R., and Tabas, I.A. (2009). Macrophage deficiency of p38alpha MAPK promotes apoptosis and plaque necrosis in advanced atherosclerotic lesions in mice. J. Clin. Invest. *119*, 886–898.

Sekiya, M., Osuga, J., Nagashima, S., Ohshiro, T., Igarashi, M., Okazaki, H., Takahashi, M., Tazoe, F., Wada, T., Ohta, K., et al. (2009). Ablation of neutral cholesterol ester hydrolase 1 accelerates atherosclerosis. Cell Metab. *10*, 219–228.

Sun, L., Wang, H., Wang, Z., He, S., Chen, S., Liao, D., Wang, L., Yan, J., Liu, W., Lei, X., and Wang, X. (2012). Mixed lineage kinase domain-like protein mediates necrosis signaling downstream of RIP3 kinase. Cell *148*, 213–227.

Tabas, I. (2010). Macrophage death and defective inflammation resolution in atherosclerosis. Nat. Rev. Immunol. *10*, 36–46.

Tabas, I., Marathe, S., Keesler, G.A., Beatini, N., and Shiratori, Y. (1996). Evidence that the initial up-regulation of phosphatidylcholine biosynthesis in free cholesterol-loaded macrophages is an adaptive response that prevents cholesterol-induced cellular necrosis. Proposed role of an eventual failure of this response in foam cell necrosis in advanced atherosclerosis. J. Biol. Chem. *271*, 22773–22781.

Thorp, E., Li, G., Seimon, T.A., Kuriakose, G., Ron, D., and Tabas, I. (2009). Reduced apoptosis and plaque necrosis in advanced atherosclerotic lesions of Apoe-/- and Ldlr-/- mice lacking CHOP. Cell Metab. *9*, 474–481.

Trichonas, G., Murakami, Y., Thanos, A., Morizane, Y., Kayama, M., Debouck, C.M., Hisatomi, T., Miller, J.W., and Vavvas, D.G. (2010). Receptor interacting protein kinases mediate retinal detachment-induced photoreceptor necrosis and compensate for inhibition of apoptosis. Proc. Natl. Acad. Sci. USA *107*, 21695–21700.

Tupin, E., Nicoletti, A., Elhage, R., Rudling, M., Ljunggren, H.G., Hansson, G.K., and Berne, G.P. (2004). CD1d-dependent activation of NKT cells aggravates atherosclerosis. J. Exp. Med. *199*, 417–422.

Welz, P.S., Wullaert, A., Vlantis, K., Kondylis, V., Fernandez-Majada, V., Ermolaeva, M., Kirsch, P., Sterner-Kock, A., van Loo, G., and Pasparakis, M. (2011). FADD prevents RIP3-mediated epithelial cell necrosis and chronic intestinal inflammation. Nature.

Zhang, D.W., Shao, J., Lin, J., Zhang, N., Lu, B.J., Lin, S.C., Dong, M.Q., and Han, J. (2009). RIP3, an energy metabolism regulator that switches TNF-induced cell death from apoptosis to necrosis. Science *325*, 332–336.